Silica gels from aqueous silicate solutions

26

Silica Gels from Aqueous Silicate Solutions

Combined ^{29}Si NMR and Small-Angle X-ray Scattering Spectroscopic Study

Peter W. J. G. Wijnen[1], Theo P. M. Beelen, and Rutger A. van Santen*

Schuit Institute of Catalysis, Eindhoven University of Technology, P.O. Box 513, 5600 MB Eindhoven, The Netherlands

The use of modern spectroscopic techniques in the study of the formation of aqueous silica gels is described. The oligomerization process of monomeric silicic acid was studied by silicon-29 NMR spectroscopy; at high pH values cyclic trimeric silicate species were favored compared to the linear structure. Aggregation of primary silica particles of molecular size (<1 nm) was studied by analysis of small-angle X-ray scattering patterns. All systems studied (pH 4.0) indicate reaction-limited aggregation. Polyvalent cations influence the rate of aggregate formation in a negative way: aluminum at low concentrations (1 mol %) significantly inhibits aggregation. A new model for the aging process that proposes that monomeric silicic acid is transported (via solution) from the periphery of the aggregate into the core of the solution is given.

THE FORMATION OF AMORPHOUS SILICA GELS is an important process in modern industry because of their many applications. Most investigations in the field of silica gel preparation have contributed to the development of a physical chemical understanding of silica gel formation. As such, many

[1]Current address: Experimental Station, DuPont (Nederland) B. V., P.O. Box 145, 3300 AC, Dordrecht, Netherlands.
*Corresponding author

0065–2393/94/0234–0517$08.00/0

procedures to synthesize silica gels tailor-made to the demands of specific applications have resulted (*1*).

Although much phenomenological and empirical knowledge is available, the polymerization process is still lacking in molecular chemical descriptions (*1–3*). The preparation of silica has more or less become an art rather than a science based on fundamental knowledge of the preparation conditions. Insights into the underlying principles and molecular chemical aspects of silica gel formation are still limited. Understanding of the molecular chemical aspects of silica gel formation is required because small variations in preparation conditions and precursor solutions can result in different structural properties of the final product. Furthermore, the molecular aspects of silica gel formation also play a role in the synthesis of crystalline, microporous silicates and aluminosilicates (zeolites) (*4*), a process still poorly understood.

This chapter presents in situ spectroscopic investigations on the formation of silica gels from aqueous silicate solutions. The processes discussed deal with (1) the formation and growth of primary particles by polycondensation of small (monomeric) silicate anions, studied by silicon-29 NMR spectroscopy; (2) the aggregations of these primary particles into ramified silica aggregates and the role of cations in the aggregation process, studied by small-angle X-ray scattering (SAXS); and (3) the reconstruction of silica aggregates through chemical processes, studied with both silicon-29 NMR spectroscopy and SAXS. These three processes can be regarded as the key processes in formation of silica gels, and as such this chapter addresses the need for a more fundamental description of the process of silica gel formation.

Silicon-29 NMR Spectroscopy

Most commercial production processes of silica gel make use of aqueous silicate solutions. In contrast to alcoholic precursor solutions previously used to study the hydrolysis and oligomerization processes of the monomeric precursor (*2*), aqueous silicate solutions (water glass) contain a broad spectrum of structurally different silicate species, all present as essentially dissolved silica. To probe the local atomic environment of silicon nuclei and investigate the degree of polymerization of silicate species, silicon-29 NMR spectroscopy has been applied since the early 1970s (*5*). The large number of structurally different silicate species observed by ^{29}Si NMR spectroscopy contributes to the fact that the observed resonance lines of commercial water-glass solutions are rather broad: overlapping and small differences in resonance frequency of the different lines cause substantial line broadening. More alkaline solutions of aqueous silicate give rise to better resolved spectra (*6*). Furthermore, the concentration of small oligomeric and monomeric silicate anions is increased with respect to the

concentration of these anions in silicate solutions of lower alkalinity as a consequence of the higher alkalinity. Increasing pH values give rise to more depolymerized species.

Oligomerization of Aqueous Monomeric Silicic Acid. Because polymerization of the water-glass solution gives rise to a broad distribution of silicate anions and thus results in poorly resolved ^{29}Si NMR lines, the application of ^{29}Si NMR spectroscopy in this type of reaction provides minor information about the different oligomerization steps and the reaction mechanism of monomeric silicic acid. Therefore a different approach to the study of aqueous silicate solutions was applied. Because of the slow dissolution of amorphous silica gel in alkaline solutions, a gradual increase in the concentration of monomeric silicic acid can be expected. In Figure 1, typical NMR spectra of such a dissolution process are presented. In this example, amorphous, pyrogenic silica gel (Aerosil 200; Degussa) was dissolved in aqueous tetramethylammonium hydroxide (TMAOH; Janssen Chimica). TMAOH was chosen as the base because silicate species present in aqueous tetramethylammonium silicate solutions show a high degree of monodispersity: the number of different silicate species is rather small compared to alkali metal silicate solutions (*7*), and this choice facilitates identification of oligomers and oligomerization pathways. Initially (Figure 1a) a single resonance line is observed, which is attributed to monomeric silicate anions. Because of the gradual dissolution of the amorphous gel matrix, an increase in monomeric silica concentration is detected. Once a certain concentration of monomeric silicic acid has been reached, oligomerization of the monomers occurs and is reflected in the occurrence of a second resonance line. This line corresponds to dimeric silicate species. Further oligomerization takes place as a result of ongoing monomer dissolution.

From the development of resonance lines in the different spectra, a qualitative reaction mechanism can be extracted for the oligomerization process. In this mechanism, formation of cyclic structures is a predominant phenomenon. In the presence of TMA cations, no linear trimeric silicate anions are found in the silicate solutions, as can be deduced from Figures 1d through 1h. The use of alkali metal hydroxides as bases shows, aside from the cyclic trimeric silicate anion, the linear structure; the relative concentration of each depends on the alkalinity and the alkali metal used. The formation of cyclic trimeric silicate anions occurs before formation of the linear trimeric species (*6*). The formation of double-cyclic silicate anions can be observed in Figure 1e; two cyclic trimeric silicate anions combine to form the prismatic hexameric silicate anion (Q^3_6). This prismatic hexameric silicate anion forms, through addition of two monomers or one dimer, the well-known cubic octameric silicate anion. This cubic octameric silicate anion has been proposed to be predominantly

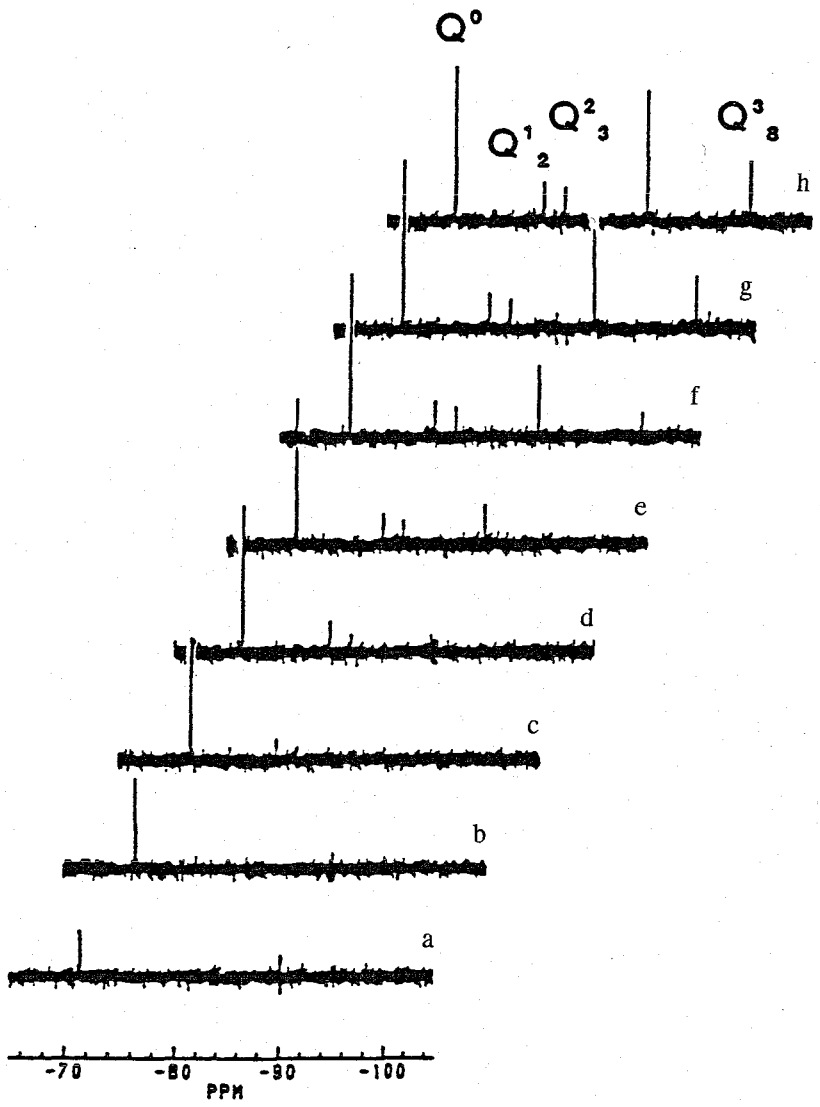

Figure 1. Dissolution of amorphous silica gel in aqueous tetramethylammonium hydroxide ($TMA_2O:SiO_2:36H_2O$) after (a) 83, (b) 250, (c) 833, (d) 1083, (e) 1250, (f) 1500, (g) 1666, and (h) 1833 min from initial mixing. The initially highly viscous suspension of tetramethylammonium silicate was introduced in zirconia magic-angle spinning NMR rotors and analyzed with a Bruker CXP-300 NMR (7.05) spectrometer. Five hundred free-induction decays were averaged that applied 45° pulses with a 10-s pulse delay. Magic-angle sample spinning was applied to average any chemical shift anisotropy arising from the highly viscous suspension.

stabilized by the tetramethylammonium cation. However, here it is shown that aside from stabilization of the Q^3_8 anion by TMA, other cyclic structures such as Q^3_6 and Q^2_3 are preferentially formed in aqueous silicate solutions containing tetramethylammonium cations. The observation that tetramethylammonium cations direct the oligomerization pathway may well be linked with the observation that during zeolite synthesis the zeolite structure needs to be built in a certain well-defined fashion. Cations in general will have an effect on the way oligomerization proceeds in aqueous silicate solutions.

Influence of Alkali Metal Hydroxides on Dissolution Rate. In a study (6) of the dissolution of amorphous silica gels in aqueous alkali metal hydroxides, the rate of dissolution was found to depend on the cation used in the dissolution reaction. A maximum in dissolution rate was found for potassium hydroxide solutions, whereas both intrinsically smaller and larger cations (lithium–sodium and rubidium–cesium) showed slower dissolution rates, as can be concluded from the concentration of dissolved silicate species (normalized peak areas) as a function of alkali metal cation (Figure 2). This result is contradictory to the expectation that a monotonic increase or decrease in dissolution rate is to be observed for the different cations used. One major effect that occurs at the high pH values of this study is that the majority of silanol groups (≡Si–OH) at the surface of the silica gel are ionized by hydroxyl anions present in the highly alkaline solution. This result implies that a large surface charge will be present on the silica. Because in aqueous solutions at high pH values contra-ions (cations) for the hydroxide (normally sodium) are present, the negative surface charges will be compensated by (alkali metal) cations.

Because the only variable changed in this dissolution study was the type of alkali metal hydroxide, differences in dissolution rate must be attributed to differences in adsorption behavior of the alkali metal cations. The affinity for alkali metal cations to adsorb on silica is reported (*8*) to increase in a continuous way from Cs^+ to Li^+, so the discontinuous behavior of dissolution rate cannot simply be related to the adsorption behavior of the alkali metal cations. We ascribe the differences in dissolution rate to a promoting effect of the cations in the transport of hydroxyl anions toward the surface of the silica gel. Because differences in hydration properties of the cations contribute to differences in water bonding to the alkali metal cations, differences in local transport phenomena and water structure can be expected, especially when the silica surface is largely covered by cations. Lithium and sodium cations are known as water structure formers and thus have a large tendency to construct a coherent network of water molecules in which water molecules closest to the central cation are very strongly bonded; slow exchange (compared to normal water diffusion) will

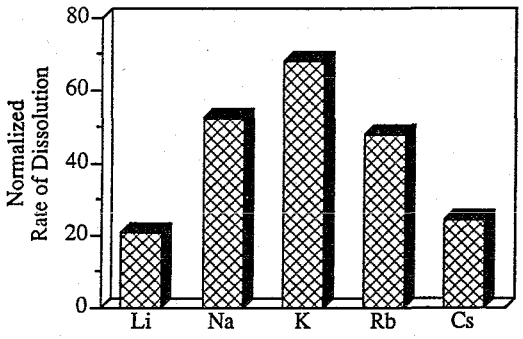

Figure 2. Normalized rate of dissolution of amorphous silica gel in alkali metal hydroxides as determined from the initial, integrated peak area of dissolved species (5 wt % silica suspensions; $M_2O:3SiO_2:180H_2O$). Other experimental details are given in the caption of Figure 1.

take place between water molecules in the nearest hydration shell and the bulk water molecules.

On the other hand, cesium, rubidium, and, to a lesser extent, potassium are known as water structure breakers; they cause the water molecules to be very disordered around the central cation. These larger cations have a small tendency to coordinate water molecules in a hydration shell, so lithium cations interact strongly with the (inner) hydration shell, whereas cesium cations barely have a hydration shell. As adsorption of (hydrated) cations will take place for aqueous silicate dispersions at high pH values, the state in which the adsorbed cations are present at the surface is crucial for promoting effects. Strong hydration forces (lithium) give rise to a slow exchange of water (hydroxyl) molecules, whereas no hydration (cesium) results in slow exchange as well. Potassium is the most favored alkali metal cation in transport reactions of hydroxyl anions towards the silica gel surface.

This phenomenon was confirmed by the introduction of symmetric tetraalkylammonium hydroxides in the dissolution of silica gel. In TMAOH the observed rate of dissolution was slow compared to the rate observed for cesium hydroxide dispersions, and cesium hydroxide has the lowest rate for the different alkali metal hydroxides. Results in Figure 3 clearly reveal an inhibition time between mixing of the silica gel with the aqueous TMAOH and the onset of dissolution. This observation is attributed to the strong interaction of the rather apolar TMA cation with the negatively charged silica gel surface. Because in this case no hydration shell is present, dissolution only occurs very slowly. The observed inhibition period of the dissolution reaction can be related to specific interactions of TMA cations with relatively large oligomeric species of the monomeric

silicic acid. From the time that prismatic hexameric silicate anions (double three-membered ring, Q^3_6) are present in the solution (*see* Figure 1e; $\delta = -89.2$ ppm), TMA cations migrate from the silica surface to the solution; this migration leaves an almost noncovered silica gel surface, and dissolution occurs as fast as in alkali metal hydroxide solutions. A speculative model for the increased affinity of TMA cations for the silicate solution is provided by the clathrate structure of TMA silicate solutions. In this model, oligomers of silicic acid (cubic octameric silicate) are surrounded by tetramethylammonium cations in such a way that the geometric nature of the silicate oligomer matches the structure of the hole induced by the arrangement of TMA cations (*9*).

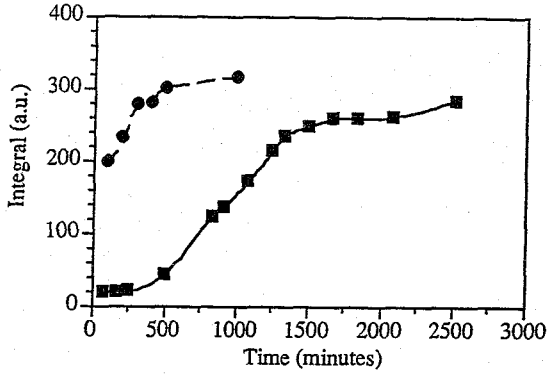

Figure 3. Total amounts of dissolved silicate anions (in terms of integrated peak area; a.u., arbitrary units) in solutions of cesium silicate (dashed line) and tetramethylammonium silicate as a function of reaction time (TMA_2O or $Cs_2O{:}3SiO_2{:}180H_2O$). The temperature was 25 °C; other experimental details are given in the caption of Figure 1.

Small-Angle X-ray Scattering

Silicon-29 NMR spectroscopy has thus been used to investigate the oligomerization of aqueous monosilicic acid. Prolonged polymerization of aqueous silicate solutions, however, yields a very broad distribution of polysilicic anions and colloidal structures (*6, 7*). This fact implies that with ^{29}Si NMR spectroscopy, only information with little detail on the ongoing polymerization process can be obtained, and so the polymerization process can be described only in a qualitative way in terms of relative changes in NMR line intensities and line widths. Therefore, a different spectroscopic technique was applied to study silica gel formation: small-angle X-ray scattering (SAXS) (*10*). As in X-ray diffraction, interference of scattered X-rays allows the identification of structural properties. From Bragg's

relation ($n\lambda = d \sin 2\theta$; λ is the wavelength, d is the interatomic separation, 2θ is the angle between the incident and diffracted light, and n is an integer), it can be seen that large structural features should be investigated at relatively small scattering (diffraction) angles (typically $2\theta < 5°$). Systems containing colloidal or subcolloidal particles can be studied at small scattering angles. Silica gels are constructed of a continuous network of particles of colloidal size (typically 3–50 nm in diameter). In the early 1980s, silica gels prepared from alcoholic precursor solutions (in contrast to the aqueous solutions discussed here) yielded scattering curves that were indicative of the formation of fractal structures (*11*).

Fractal Behavior in Silica Gel Chemistry. In fractal theory a structure can be described in terms of its fractal or broken dimensionality (*12*). This dimensionality, in contrast to the Euclidean dimensionality, which quantifies the space dimensionality embedding the structure, often has a noninteger value between 1 and 3. Fractal structures do not have a constant value for density; it gradually changes when traversing the system. For mass fractals, the way in which density varies is reflected in the fractal dimensionality D: density ρ varies with length scale r according to $\rho \propto r^{D-3}$. The fractal dimensionality can be used as a kind of fingerprint in the description of the process of aggregation of primary silica particles: different types of aggregation process result in different fractal dimensionalities (*13*).

Fractal behavior is reflected in a power-law relationship between scattered intensity I and scattering vector $\mathbf{Q}$ ($\mathbf{Q} = 2\pi/\lambda \sin 2\theta$). Therefore, in a log–log plot of scattered intensity versus scattering vector, fractality is observed as a linear region of the scattering curve; the slope of this linear part is, in general, smaller than 3 if the material is fractal with respect to the mass (variation of density within the structure) and between 3 and 4 if the material is fractal with respect to the surface area (*13–15*). In Figure 4, a computed small-angle scattering curve of a fractal system is presented (*16*). From deviations from power-law scattering at small and large scattering vectors, information is extracted concerning the size of the fractal aggregates and the size of the primary particles constructing the aggregate, respectively. These two parameters determined from in situ small-angle scattering curves are the structural properties that are determined by aggregation kinetics imposed by the precursor composition. A continuous increase in size of the silica aggregates was observed during the formation of silica gel (*17*). Moreover, after reaching the gelation point, the aggregate size still appears to increase as a function of time. At the gelation point, a continuous percolating network of silica particles exists in the solution, which has an infinite viscosity: twisting of the reaction vessel does not deform the meniscus.

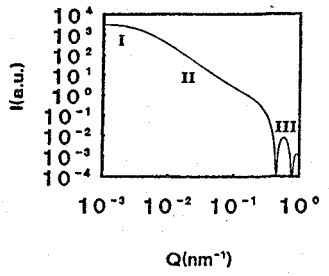

Figure 4. Simulated small-angle scattering curve from fractal geometry theorems (16). The small-angle scattering curve represents scattering from a fictitious fractal aggregate (R = 250 nm, D = 2.25, and the size of the primary building unit r_0 was 3 nm).

According to classical theories of gelation, a continuous aggregate of infinite size should be present at the gelation point. However, from the SAXS curves a determinable, finite size of the aggregates is extracted. This observation suggests that the growth process of silica aggregates has to be anisotropic. The finite size of fractal silica aggregates in silica gels might indicate the presence of elongated, intermingled structures with a finite (mean) aggregate radius. On the other hand, according to Martin and Hurd (*14*), SAXS on gelated, nondilute silica systems gives no information about the size of the aggregates, and so no conclusion should be drawn from the development of aggregate size at relatively long reaction times. From a certain reaction time near the gelation point, the solutions can no longer be considered dilute, so determination of aggregate sizes becomes disputable. However, this chapter focuses on qualitative differences in the evolution of aggregate size at reaction times that are short compared to the gelation time.

The size of primary particles can be extracted from the deviation of fractal behavior at large scattering vectors **Q**. In silica gels freshly formed from aqueous silicate solutions, no deviation from this fractal power law could be observed for **Q** values as high as 2 nm^{-1}. This result implies that the primary particles of freshly prepared silica gels are smaller than 2 mm, maybe even of molecular size. Oligomers present in the aqueous silicate solutions used as precursor solutions are not subject to further growth in acidic solutions, but merely aggregate into continuous networks of silicate particles. At low pH values (pH ≈ 4) aggregation of oligomers is a fast process in relation to growth of the primary particles.

Influence of Total Silica Concentration on Aggregation Kinetics. Dilution of the silicate solution would be expected to give rise to a crossover in the type of aggregation behavior of the primary silicate particles. For relatively concentrated systems ($[SiO_2]$ ≈ 5 wt %), a

reproducible fractal dimensionality of $D = 2.20 \pm 0.05$ was measured (Figure 5). This value of the fractal dimensionality is in fairly good agreement with fractal dimensionalities obtained from computer simulations of reaction-limited cluster–cluster aggregation (*13*). In this limiting situation of reaction-limited aggregation, diffusion of particles or clusters of particles toward each other is faster than the kinetics of the chemical reaction between the particles. Dilution of the silicate solution in aggregating particles (total silica concentration) should therefore result in an increasing importance of the diffusion rate of the aggregating particles. So *reaction*-limited aggregation should change into *diffusion*-limited aggregation, as was observed by Aubert and Cannell (*18*) for colloidal silica solutions. This transition in type of kinetic aggregation process is accompanied by a difference in fractal dimensionality. Experimentally, however, no influence of the total silica concentration ($0.1 < [SiO_2] < 8$ wt %) on the fractal dimensionality was observed at the length scales (1–30 nm), temperature, and time scales investigated (Figure 5). This result implies that diffusion of particles in the aqueous silicate solution or suspension must be a fast process compared to the reaction kinetics between two aggregating particles, or internal organizations must be fast compared to aggregation. Concentrations lower than 0.1 wt % do not lead to aggregation processes.

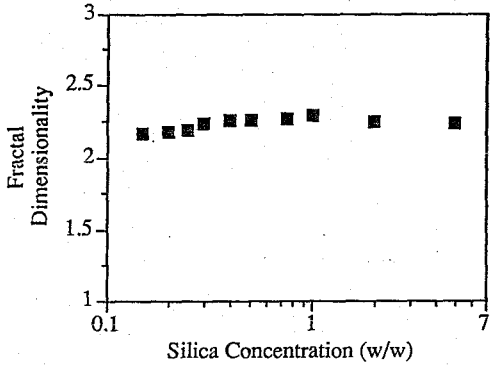

Figure 5. Fractal dimensionality of aqueous silica aggregates differing in total silica concentration obtained from SAXS spectra. The spectra were recorded after 5 days of reaction (pH 4.0 at 25 °C) in sealed polyethylene bottles. SAXS spectra were recorded at the Synchrotron Radiation Source of Daresbury Laboratories, United Kingdom, on beam line 8.2.

In contrast with these observations concerning the independence of fractal dimensionality from monomeric silicate concentration, the remarkable observation was made that the presence of oligomeric silicate anions

increases the rate of aggregate formation considerably (*17*). A decrease in the pH value of precursor solutions low in silica concentration (about 0.2 wt %), gives rise to oligomerization of the monomeric silicate anion. The oligomers formed appear to act as aggregation kernels for the silicate anions. The presence of these aggregation kernels induces rapid aggregation, as is reflected in the fractal dimensionality of the aggregates. Compared with usually observed fractal dimensionalities of aqueous silicate aggregates ($D = 2.2$), the fractal dimensionality of aggregates grown in solutions of low silica concentration and in the presence of oligomers is low ($D = 1.8$). This low fractal dimensionality points to a diffusion-limited cluster–cluster aggregation process. Reorganizations in the structural arrangement of the primary building units gradually cause an increase in fractal dimensionality to values observed for the reaction-limited cluster–cluster aggregation type (*19, 20*).

Influence of Polyvalent Cations on Aggregation Kinetics. This influence was investigated. No influence on the final fractal dimensionality of the gelating silicate solutions was observed for the cations investigated (Li^+, Na^+, K^+, Rb^+, Cs^+, TMA^+, Mg^{2+}, and Al^{3+}). The rate of aggregate growth, however, does strongly depend on the presence of polyvalent cations and hydrophobic monovalent cations (TMA) (*21*). Aggregation is retarded by addition of aluminum cations (Al:Si = 0.01) and to some lesser extent by addition of magnesium cations (Figure 6). This difference is understood in terms of the valency of the cations. Investigation of the influence of different concentrations of aluminum cations revealed that increasing aluminum concentrations cause the observed inhibition with respect to aggregate growth to diminish (Figure 7). Fast reaction between aluminum cations and silicate oligomers causes the silica particles to become charge stabilized. Aggregation is slow because of the charges of the primary particles. The structure of the aggregates is such that in a model of screened aggregation, initially low dimensionalities are observed. However, when the concentration of aluminum is increased, formation of homogeneous aluminosilicates causes charge stabilization to decrease. The aggregation kinetics resemble kinetics in solutions with no aluminum cations added.

Addition of tetramethylammonium cations results in an increase in aggregation rate, which can be attributed to the breaking of the local structure of water molecules surrounding the silicate particles. The activation energy of reaction between two primary particles is decreased.

Aging of Aqueous Silica Gels

So far, a discussion on the processes involved in the formation of silica gels has been presented. However before a silica gel, with its intrinsic

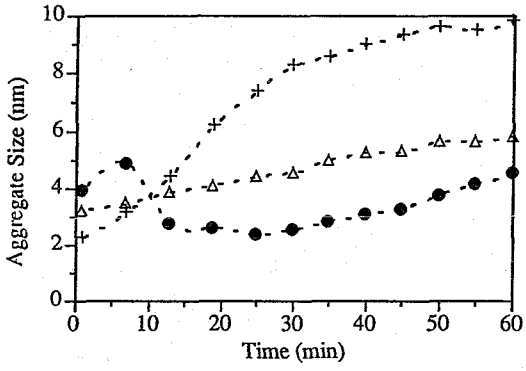

Figure 6. Size of aggregates as a function of reaction time for silicate solutions containing different cations: +, K only; Δ, Mg:Si = 0.01 mol/mol; ●, Al:Si = 0.01 mol/mol. The total concentration of silica was 5 wt %. Silica gels were prepared at pH 4.0 at room temperature (25 °C) by adding the silicate solution under vigorous stirring to a solution of hydrochloric acid (2 N) containing $MgCl_2$ or $Al_2(SO_4)_3$.

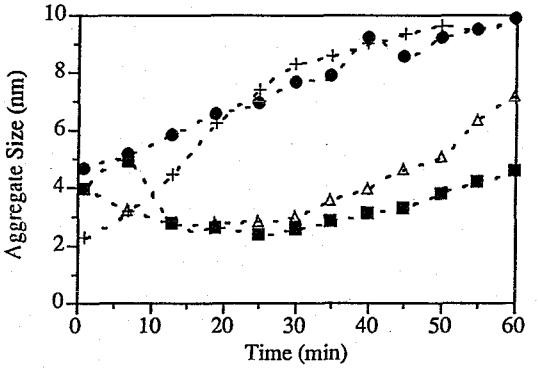

Figure 7. Size of aggregates as a function of reaction time for silicate solutions containing different concentrations of aluminum cations: +, K only, Al:Si = 0.0; ■, Al:Si = 0.01; Δ, Al:Si = 0.04; and ●, Al:Si = 0.10. The pH was 4.0, and the temperature was 25 °C. The total concentration of silica was 5 wt %. Silica gels were prepared at pH 4.0 at room temperature (25 °C) by adding the silicate solution under vigorous stirring to a solution of hydrochloric acid (2 N) containing different concentrations of $Al_2(SO_4)_3$.

properties of high specific surface area preserved, can be made, it must be aged in a way that prevents the framework of silica particles from collapsing upon drying. Until now, aging of aqueous silica gels was considered an Ostwald dissolution process of silicate units at surfaces with small radius of curvature (small particles) and subsequent deposition at surfaces with large or negative radius of curvature (large particles and

necks between particles, respectively) (*1*, p 228). In Figure 8, small-angle scattering curves of a freshly prepared and an aged aqueous silica gel are presented; different scattering characteristics are evident. In the scattering profile in Figure 8b, the scattering of primary particles can be distinguished (part III in Figure 2) from the case of freshly prepared silica gels, for which no scattering of primary particles can be observed (Figure 8a). Thus, the mean size of the scattering primary particles increases during aging from molecular level (<0.5 nm) to colloidal level (ca. 3–5 nm). The fractal dimensionality on the other hand has changed to a value smaller than the initial fractal dimensionality, so the gradient in density within the aggregates has become larger. Here dissolution is presumed to preferentially occur at peripheral positions in the aggregates, where the density in silica is low compared to the more dense core of the aggregates. Subsequent deposition of the monomeric species in the core of the aggregates causes the difference in density between the core (high) and the peripherals (low) to increase; a decrease in fractal dimensionality results.

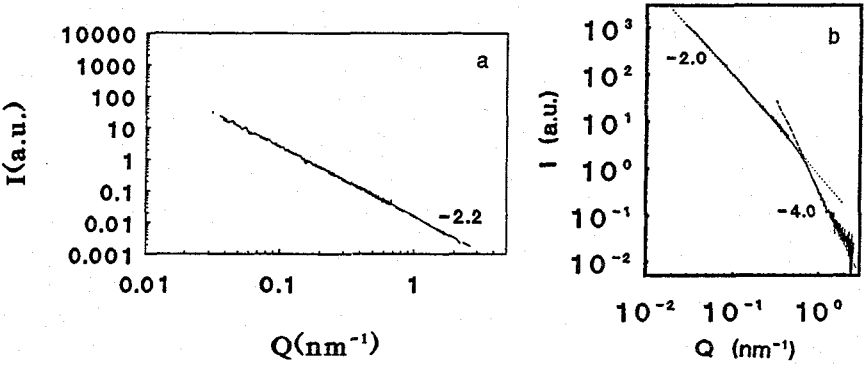

Figure 8. SAXS curves of a silica gel prepared at pH 3.9 from potassium water glass and hydrochloric acid: a, freshly prepared silica gel recorded after 2 h of reaction; b, same gel as in a, but after 1 year of aging at room temperature. The dotted line is a nonlinear least-squares fit of the fractal region in the curve and gives $D = 2.0$. *The dashed line is from the Porod law* ($I \propto Q^{-4}$). *In both a and b, two scattering curves measured at two different camera lengths (4.5 and 0.7 m) are combined to cover a broad scattering range (2 orders of magnitude in* Q *vector).*

The driving force for structure transformation can be related to the entropy of the structures (22). Very open structures are of highest entropy and thus will strive for a state that has less entropy. Because the structure of the silica aggregates is more or less rigid, the only way to decrease entropy is to gradually dissolve silica at places of highest entropy (i.e., the

low-density peripherals of the fractal structures) and to deposit the dissolved monomers at places with higher density (i.e., lower entropy). An increase in solubility of the silica aggregates will contribute to a faster process of structure reorganization. As such, aging of aqueous silica gels can be accelerated by higher pH values, high temperatures, and the presence of fluorine anions (*20*). The rate of dissolution of monomeric silicate anions is rate determining in the aging processes of aggregates formed by reaction-limited cluster–cluster aggregation. Interestingly, aging of aggregates formed by reaction-limited aggregation gives a decrease in fractal dimensionality with an increase in primary particle size. Aging of aggregates formed by diffusion-limited cluster–cluster aggregation results in an increase of fractal dimensionality at (nearly) constant primary particle size (*20*). The time scales on which both transformations take place are very different. Aging of aggregates grown by diffusion-limited aggregation is fast compared to aging of reaction-limited aggregates. Both transformations correspond to a decrease in system entropy and potential energy.

References

1. Iler, R. K. *The Chemistry of Silica*; Wiley: New York, 1979.
2. Brinker, C. J.; Scherer, G. W. *Sol Gel Science*; Academic: Boston, MA, 1990.
3. Hench, L. L.; West, J. K. *Chem. Rev.* **1990,** *90*, 33.
4. Barrer, R. M.; Coughlan, B. *Molecular Sieves*; Society of Chemical Industry: London, 1968.
5. Engelhardt, G.; Jancke, H.; Mäge, M.; Pehk, T.; Lippmaa, E. *J. Organometallic Chem.* **1971,** *28*, 293.
6. Wijnen, P. W. J. G.; Beelen, T. P. M.; De Haan, J. W.; Rummens, C. P. J.; Van de Ven, L. J. M.; Van Santen, R. A. *J. Non-Cryst. Solids* **1989,** *109*, 85.
7. Wijnen, P. W. J. G.; Beelen, T. P. M.; De Haan, J. W.; Van de Ven, L. J. M.; Van Santen, R. A. *Colloid Surf.* **1990,** *45*, 255.
8. Depasse, J.; Watillon, A. *J. Colloid Interface Sci.* **1970,** *33*, 430.
9. Keijsper, J. J.; Post, M. F. M. In *Zeolite Synthesis*; Occelli, M. L.; Robson, H. E., Eds.; Symposium Series 398; American Chemical Society: Washington, DC, 1989; pp 28–48.
10. Guinier, A.; Fournet, G. *Small Angle Scattering of X-rays*; Wiley: New York, 1955.
11. Brinker, C. J.; Keefer, K. D.; Schaefer, D. W.; Ashley, C. S.; Assink, R. A.; Kay, B. D. *J. Non-Cryst. Solids* **1982,** *48*, 47.
12. Mandelbrot, B. B. *The Fractal Geometry of Nature*; W. H. Freeman and Co.: San Francisco, CA, 1982.
13. Meakin, P. *Adv. Colloid Interface Sci.* **1988,** *28*, 249.
14. Martin, J. E.; Hurd, A. J. *J. Appl. Cryst.* **1987,** *20*, 61.
15. Schmidt, P. W. In *The Fractal Approach to Heterogeneous Chemistry*; Avnir, D., Ed.; Wiley: New York, 1989.
16. Teixeira, J. *J. Appl. Cryst.* **1988,** *21*, 781.
17. Wijnen, P. W. J. G. Ph.D. Thesis, Eindhoven University of Technology, Eindhoven, the Netherlands, 1990.
18. Aubert, C.; Cannell, D. S. *Phys. Rev. Lett.* **1986,** *56*, 738.

19. Wijnen, P. W. J. G.; Beelen, T. P. M.; Rummens, C. P. J.; Saeijs, J. C. P. L.; Van Santen, R. A. *J. Appl. Cryst.* **1991**, *24*, 759.
20. Wijnen, P. W. J. G.; Beelen, T. P. M.; Rummens, C. P. J.; Saeijs, J. C. P. L.; Van Santen, R. A.; *J. Colloid Interface Sci.* **1991**, *145*, 17.
21. Beelen, T. P. M.; Wijnen, P. W. J. G.; Rummens, C. P. J.; Van Santen, R. A. In *Better Ceramics through Chemistry IV*; Zelinski, B. J. J.; Brinker, C. J.; Clark, D. E.; Ulrich, D. R., Eds.; *Mat. Res. Soc. Symp. Proc*; Materials Research Society: San Francisco, CA, 1990; Vol. 180; pp 273–276.
22. Kaufman, J. H.; Melroy, O. R.; Dimino, G. M. *Phys. Rev. A* **1989**, 39, 1420.

RECEIVED for review July 17, 1991. ACCEPTED revised manuscript December 27, 1991.